LEACHING OF LEAD FROM SPENT MOTORCYCLE BATTERY IN HYDROCHLORIC ACID. PART I: DISSOLUTION KINETICS

A.A. Baba, F.A. Adekola, G.D. Ewuloye
Department of Chemistry, University of Ilorin, P. M. B. 1515, Ilorin-Nigeria

Received 06.09.2010
Accepted 20.11.2010

Corresponding author: A.A.Baba, E-mail: alafara@unilorin.edu.ng, Tel: +2348035010302, Fax: +234-31-221911, Department of Chemistry, University of Ilorin, P. M. B. 1515, Ilorin-Nigeria

Abstract
This paper examines dissolution kinetic data on the development of hydrometallurgical route for possible recovery of lead from spent motorcycle battery ash leached liquor in hydrochloric acid solution. The influence of acid concentration, reaction temperature, particle diameter, solid/liquid ratio and stirring rate on the dissolution rates has been investigated. The dissolution rates are greatly influenced by the reaction temperature, acid concentration, stirring rate, solid/ liquid ratio and particle diameter. In 8.42 M HCl and at 80 °C, about 82.2 % of the battery ash was dissolved within 120min using 0.050-0.063 mm particle diameter and solid/liquid ratio of 10g/L. The calculated activation energy, E_a, reaction order and Arrhenius constant from the experimental data were 36.40 kJ/mol, 0.76 and 24.53 s^{-1} respectively for the dissolution process. The kinetic data for the dissolution rates have been analyzed and were found to follow the shrinking core model for the diffusion control mechanism with surface chemical reaction as the rate determining step. Finally, the X-ray diffraction spectrum showed that about 18% of the initial solid material that constituted undissolved materials contained mainly silica (α-SiO_2).

Keywords: Leaching, dissolution, spent batteries, hydrochoric acid.

1 Introduction

A battery is an electrochemical device that basically converts chemical energy into electrical energy. It consists of an anode, a cathode, an electrolyte, separators and external case. The two basic types of batteries are primary batteries such as zinc-carbon, alkaline manganese, silver oxide and mercuric oxide; and secondary batteries such as lead-acid, nickel cadmium, nickel metal hydride and lithium ion [1]. A drawback of these type of battery is their limited lifespan; typically between six months to four years. The short life is due to internal deterioration of the lead plates which constitute the electrodes for the battery [2]. The increasing public concern about the environment in the last decade has resulted in stricter regulations worldwide, particularly those related to the disposal of hazardous residues containing heavy metals such as portable batteries including motorcycle batteries [3].

Disposal of spent batteries is of major concern to the environment in terms of heavy metals content contained therein. According to the battery market evolution of 2003, the total portable battery weight in the East and West Europe was estimated to be 164,000 tons, of which zinc-carbon and alkaline batteries constituted 30.5% and 60.3% respectively [4].

All types of materials present in a battery will contribute in some way to increase the environmental pollution. When discarded, some of them, such as carbon, are not so aggressive to

the environment and can quickly merge into the ecosystem without noticeable impact. Cadmium, lead and mercury are the heavy metal components most likely to be the target of environmental concerns [5].

Most of these materials can be technically recovered by means of mechanical and chemical treatment. The materials recovered show some advantages as they could be returned to the batteries production as raw materials or can be used for other purposes. For example, the steel scrap can be sold to steel mills, manganese could be sold to the steel industry and zinc can be used in metallurgical industries [6].

The preliminary treatment of batteries consists of sorting and dismantling. The collected batteries are first sorted by type (i.e. by chemical composition) in order to make leaching and liquid-liquid extraction operations more efficient. In the dismantling step, the spent battery dust is separated from plastic, iron scraps and paper residues which can be recycled. The dust is leached by an acidic solution in order to transfer the metals of interest from the dust to the aqueous liquor [7].

A good number of write-ups have been documented on the application of hydrometallurgical and pyrometallurgical route for kinetics and recovery of some valuable metals from various types of batteries (**Table 1**).

Table 1 Summary of some investigations on the metal recovery from various types of spent batteries

Type of battery	Leachant	Operational conditions			Inference	Reference
		Particle size	Leaching Time	Temperature		
Zn-C	4M HCl	0.050-0.063mm	120 min.	80^{0}C	90.3% dissolution; Ea of 22.8kJ/mol, 94.2% extraction efficiency, 95% Zn stripped.	[8]
Alkaline batteries	8% v/v H_2SO_4	500 µm	60 min.	80^{0}C	Co(37%), Cu(1%), Al(85%), Li(55%) leached, Co(68%) and Al(98%) extracted.	[3]
Ni-MH	2M H_2SO_4	Not given	240 min.	90^{0}C	98% rare earth recovered, with 100% Fe and 70% Zn removed via precipitation respectively.	[5]
Alkaline and Zn-C	3M H_2SO_4	500µm	300 min.	90^{0}C	94.1% and 87.3% of Mn and Zn extracted respectively.	[4]
Li-ion	4M HCl	Not given	60 min.	80^{0}C	About 100% Li, Co extracted.	[9]
Ni-Cd	4M HCl	Not given	120 min.	60^{0}C	›90% Ni , electroplated	[10]

It is evident from Table 1 that the metal ion beneficiation varies from one battery type to another. It is important to note that studies on the dissolution kinetic study on the spent motorcycle batteries, leading to its metal ions recovery have not been attempted.

Table 2 Elemental analysis of the spent batteries ashed sample by ICP-MS

Element	Pb	Zn	Mn	Fe	Nb	Ra	Cu	Ti
Concentration (%)	47.33	1.36	0.79	2.11	0.05	0.06	0.034	0.006
Element	W	Cd	Cr	Rb	Ag	Ca	S	SiO_2
Concentration (%)	0.099	0.042	0.005	0.003	0.002	0.043	0.21	13.41

*Others including Arsenic and Carbon = 6.36% and Oxygen obtained by difference = 28.09%

Pyrometallurgical and hydrometallurgical processes can be used with different energy consumption and environmental impact that generally favour the application of the second ones. Hydrometallurgical processes are generally characterized by different steps of pre-treatment followed by leaching and metal separation. The main difference among the patents lay just in the methods used to recover metals from leach liquor [21]. The high level of poverty in some developing countries, especially in sub-saharan Africa has steadily increase motorcycle consumption due to its commercial usage, which if not under control can constitute nuisance to the society. Hence, the recycling of valuable metals including lead is necessary. Therefore, this work was design to establish the dissolution kinetic parameters for subsequent extraction of metal ions from the spent motorcycle battery ash leach liquor in hydrochloric acid.

2 Experimental Procedures

The spent motorcycle battery: FORGO 3FM45, 6V, 4.5Ah was kindly supplied by Farouq Battery charger, Ipata-Oloje in Ilorin West Local Government Area of Kwara State, Nigeria. This was dismantled using a hammer mill, and the residual fine portion obtained (0.050-0.063mm) containing the metals to be recovered was ashed in a combustion furnace at a temperature of about 550^{o}C for 60 min. This is an optimum period for the completion of the ashing [8].

Characterization of the powder

The ash powder was sieved into four particle sizes and the fraction with particle diameter: 0.050-0.063mm originating from the first dismantling step were submitted to Inductively Coupled Plasma-Mass Spectrometry (ICP-MS, Yokogawa model HP-4500) and X-ray diffraction (XRD, Philips scientific) studies for qualitative and quantitative analysis.

Leaching

The dissolution experiments were investigated in a 250ml glass reactor equipped with a mechanical stirrer. For each leaching experiment, the solution mixture was freshly prepared by dissolving 1.0g of the battery ash in 100ml HCl solution temperature at 55^{0}C. The fraction of ashed sample dissolved (α) was followed at various time intervals and at various HCl concentration (0-12M). The concentration which resulted in maximum dissolution (8.42M) was subsequently used for optimization of other leaching parameters including temperature, particle size and stirring speed. The energy of activation (E_a) and rate constant were calculated from the Arrhenius plots. For all the leaching experiments, the fraction of the ashed sample dissolved were evaluated from the difference in weight of the amount dissolved or undissolved at various contact time up to 120min, after oven dried at about 60^{0}C. The post-leaching residual product at 80^{0}C after dissolution in 8.42M HCl was also subjected to X-ray diffraction examination (XRD, Philips scientific) using $Cu_{\alpha 1}$ target, 1.541Å (40kV, 55mA) [5, 6, 8].

3 Results and Discussion

3.1 Characterization of dry powder by ICP-MS and X-ray Diffraction

The results of elemental analysis of the spent motorcycle batteries ashed material are summarized in **Table 2**.

The results of chemical analysis by ICP-MS showed expressive amount of Pb, which represent 83% of the total mass of the sample. According to the X-ray spectrum (**Fig. 1**), Baumhauerite-

$Pb_3As_4S_9$ and α-quartz (SiO_2) are the major peaks found in the powder. The XRD data also revealed the presence of associated compounds such as Halotrichite-$FeAl_2(SO_4)_4.22H_2O$, Okenite-$CaSi_2O_5.2H_2O$ and carbon-C; including low amount of sodiumalum-$NaAl(SO_4)_2.12H_2O$ and sodium sulphide arsenate hydrate-$Na_3AsOS_3.11H_2O$. All these supported the results of the elemental studies by ICP-MS.

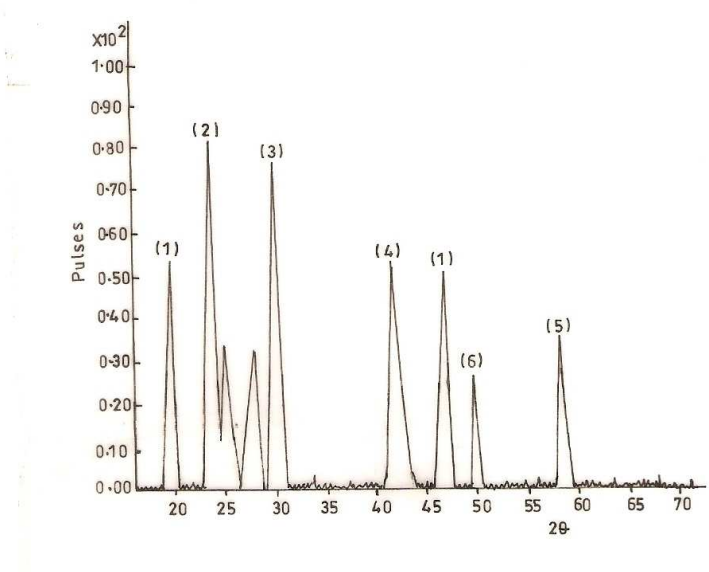

Fig.1 X-ray spectra of motorcycle battery ash with the most probable compounds identified. Joint committee on powder diffraction standard, JCPDS file No. and diffraction patterns are put in brackets. (1): α-SiO_2[46.-1045, 1 0 1]; (2): $FeAl_2(SO_4)_3.22H_2O$ [39-1387, 0 2 4]; (3,4): $Pb_3As_4S_9$[12-0281, 0 2 0]; (5): $CaSi_2O_5.2H_2$[33-0305, 0 0 1]; (6): C[41-1487, 1 0 1]

3.2 Results of Leaching Studies

Influence of Stirring Rate

The effect of stirring rate on the dissolution of battery ash sample in 8.42M HCl solution were carried out at various stirring speeds under constant conditions for 120min. **Table 3** shows the effect of stirring speed on motorcycle battery ash dissolution.

Table 3 Effect of stirring rate on battery ash dissolution in 8.42M HCl

Stirring rate, min^{-1}	Amount of battery ash dissolved (%)
0	48.16
180	61.68
270	70.35
360	79.49
450	82.23
540	82.17
630	82.17

Experimental conditions: Particle diameter = 0.050-0.063mm; Temperature = 80^0C; solid/liquid ratio =10g/L

It is evident from Table 3 that the amount of the battery ash dissolved increases with stirring speed between the range 0-450rpm. The amount dissolved appears to be practically constant

afterwards. The dissolution seems to reach a steady state at 450rpm and was subsequently kept for use. Therefore, increase in the amount of battery ash dissolved with increasing stirring speed indicates that the dissolution reaction may be controlled by diffusion.

Influence of solid/liquid ratio

The results in **Table 4** shows that the amount of battery ash dissolved increases with decrease in the solid/liquid ratio [8].

Table 4 Effect of solid/liquid ratio on battery ash dissolution for 120min

Solid/liquid ratio, g/ml	Amount of battery ash dissolved (%)
1:100	82.21
1:20	68.27
1:10	43.49
1:5	17.36

Experimental conditions:- HCl 8.42M; Stirring rate = 450rpm; Temperature = 80°C; Particle diameter = 0.050-0.063mm

The increase in solid/liquid ratio could decrease the concentration of metal ion in leaching solution, strengthen mass transfer and accelerate the leaching rate. But too high solid/liquid ratio would lead to the increase of leaching solution volume, which is not favourable to subsequent separation [11]. Therefore, solid/liquid ratio (10g/L) which gave the highest dissolution was kept for further use in this study.

Influence of HCl concentration

Fig. 2 shows that the battery ash dissolution increases gradually with leaching time and with increasing HCl concentration (0.1M - 8.42M). It is evident that above 8.42M HCl concentration, no further increase was noticed. The reason for this may be attributed to possible precipitation of metal chloride [12].

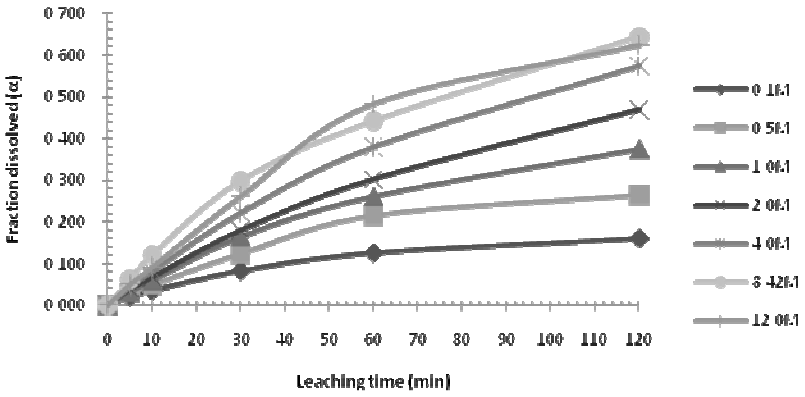

Fig.2 Fraction of battery ash dissolved vs leaching time at various concentrations of HCl
Experimental conditions: HCl concentration = 0.1M - 12M. Temperature = 55^0C; solid/liquid ratio = 10g/L; Particle diameter = 0.050-0.063mm, Stirring rate = 450rpm

Influence of temperature

The influence of temperature on the rate of battery ash dissolution is shown in **Fig. 3**.

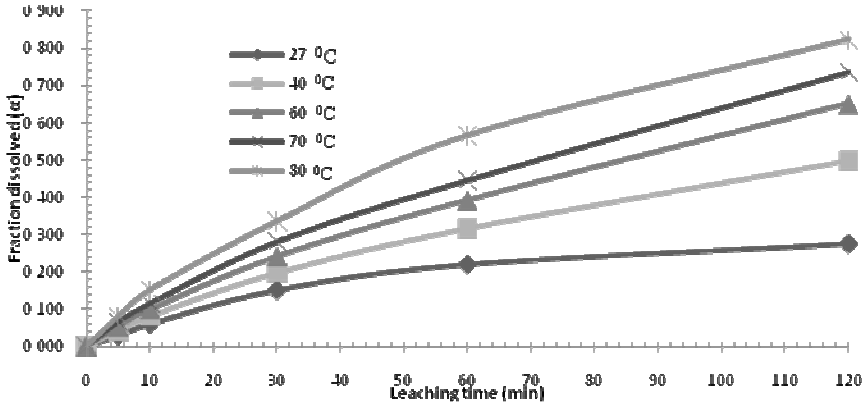

Fig.3 Influence of temperature on battery ash dissolution in 8.42M HCl

It is clearly observed that the dissolution rate increases with temperature increasing from 27 to 80°C. Hence, the HCl reactive activity is intensified greatly when temperature increases. The dissolution rate can be improved with increase in temperature. Besides, at high temperature, the operation cost increases and loss of hydrochloric acid due to evaporation [13]. So, 80^0C is chosen as an optimum temperature.

Influence of particle diameter

The influence of particle diameter on the rate of battery ash dissolution was examined. **Fig. 4** shows that the battery ash dissolution increases with leaching time and thus with decreasing particle diameter. The amount of the battery ash dissolved reached 38.57 and 82.23% after 2 hours of leaching for 0.102-0.212mm and 0.05-0.063mm particle diameter respectively.

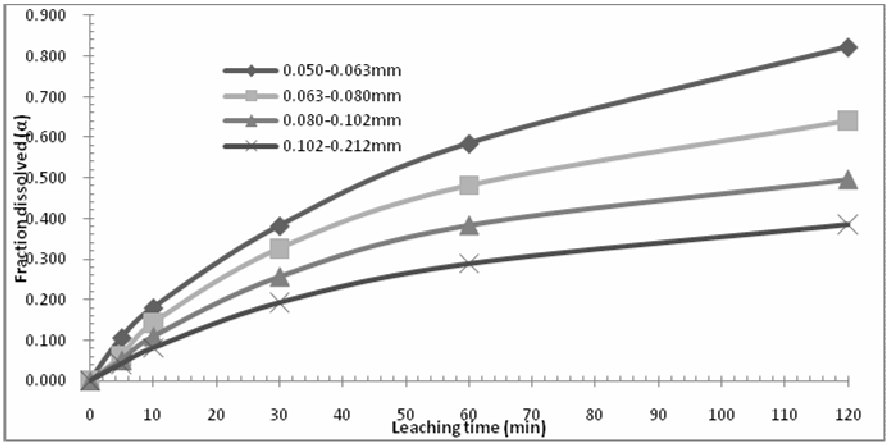

Fig.4 Influence of particle diameter on batt4ry ash dissolution in 8.42M HCl at 80^0C

3.3 Kinetic analysis

The shrinking model considers that the leaching process is controlled either by the diffusion of reactant through the solution boundary layer, or through a solid product layer, or by rate of the surface chemical reaction [14]. The simplified equations of the shrinking core model when either

diffusion or the surface chemical reactions are the slowest step can be expressed respectively as follows [15]:

$$\left[1-\frac{2}{3}\propto-(1-\propto)^{2/3}\right]=\frac{2M_B D C_A}{\rho_B a r_o^2}t=k_d t \quad (1)$$

$$\left[1-(1-\propto)^{1/3}\right]=\frac{K_c M_B C_A}{\rho_B a r_o}t=k_r t \quad (2)$$

where α is the fraction of battery ash dissolved, K_c the kinetic constant, M_B the molecular weight of the solid, C_A the concentration of the dissolved leachant A (HCl) is the bulk of the solution, a the stoichiometric coefficient of the reagent in the leaching reaction, r_0 the initial radius of the solid particle, t the reaction times, D the diffusion coefficient in the porous product layer and k_d and k_r are the rate constants respectively, which are calculated from equations (1) and (2) respectively [14]. Hence, for better understanding of the dissolution mechanism of spent battery ash by HCl solution, each of the above equations (1) and (2) was tested.

Of the two tested kinetic models of equations (1) and (2), only equation (1) fitted perfectly the data presented in Figs. 2 and 3, with good correlation and was used for the construction of the following kinetic plots.

The results on the influence of hydrogen ion concentration (from HCl), in Fig. 2 were applied to this kinetic model and K_d values and correlation coefficients for each H^+ ion concentrations were evaluated.

From the K_d and hydrogen ion concentration values, plot of ln K_d versus ln $[H^+]$ was obtained (**Fig. 5**). As seen in Fig. 5, the order of reaction with respect to hydrogen ion was proportional to 0.76, with a correlation coefficient of 0.99.

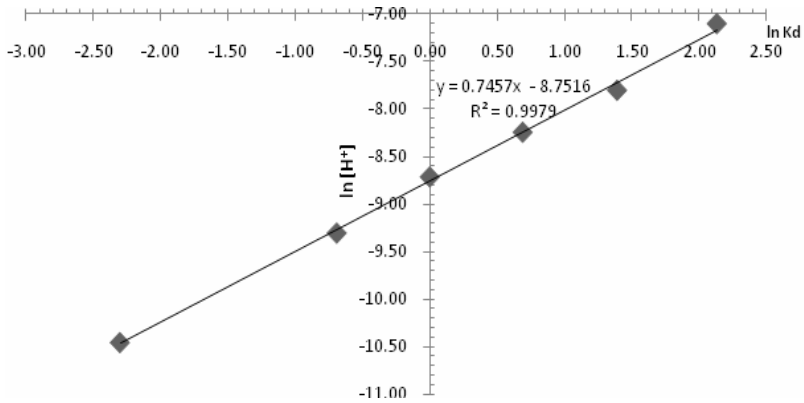

Fig.5 Plot of ln K_d vs. ln $[H^+]$
Experimental conditions:- Particle diameter = 0.050-0.063mm; Temperature = 80°C; Solid/liquid ratio = 10g/L

The application of surface diffusion kinetic model to Fig. 3 is shown in **Fig. 6**.

The apparent rate constants, K_d and K_r calculated from equations (1) and (2) respectively and their correlation coefficients for each temperature are given in **Table 5**.

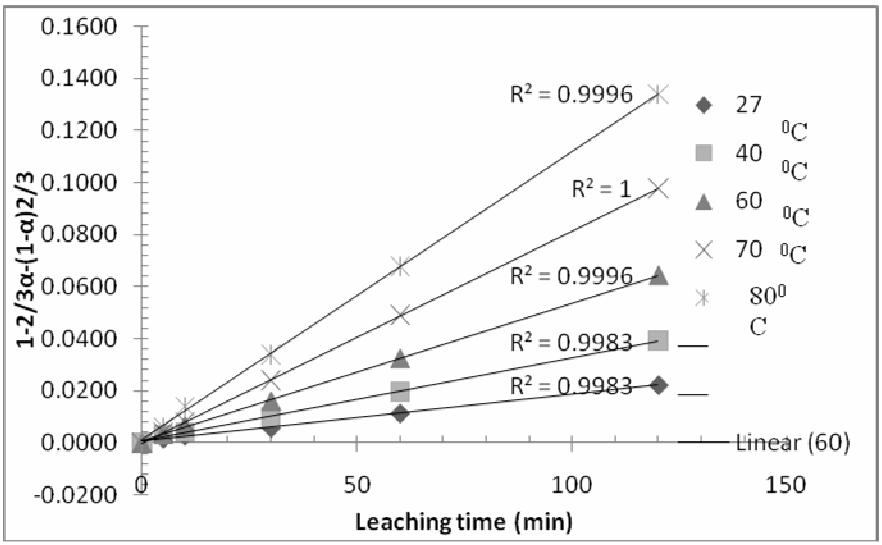

Fig.6 Plot of $1 - {}^{2}/_{3}\,\alpha - (1 - \alpha)^{2/3}$ vs leaching time at different temperatures.
Experimental conditions:- [HCl] = 8.42M; Solid/liquid ratio = 10g/L, Stirring rate = 450rpm; Particle diameter = 0.050-0.063mm

Table 5 The K_d, K_r and correlation coefficients values for different temperatures

Temperature	Apparent rate constants ($10^{-4}min^{-1}$)		Correlation coefficient (R^2)	
	K_d	K_r	K_d	K_r
27	1.801	8.417	0.998	0.842
40	2.493	16.926	0.998	0.836
60	5.361	24.417	1.000	0.892
70	8.162	29.667	0.994	0.859
80	11.101	36.251	0.999	0.895

From **Fig. 6**, the Arrhenius plot considering the apparent rate constants was evaluated by applying equation (1) to leaching experimental data (**Fig. 7**). The calculated activation energy, E_a, for the dissolution process was 36.40 kJ/mol, suggesting diffusion controlled mechanism. The dissolution result of an ash layer developing around the unreacted core. This diffusion control rate is slower than the chemical reaction control rate. The diffusion is a result of an ash layer developing around the unreacted core. This diffusion control rate is slower than the chemical reaction control rate. The reaction might proceed from the particle by leaching in an apparatus such as an attrition mill [16].

Furthermore, a value of $24.53s^{-1}$ was subsequently obtained for the Arrhenius constant and with a corresponding correlation coefficient of 0.998 from a replot of Fig. 7 on the extended scale comprising the origin.

Since the calculated activation energy from Fig. 7 seems to suggest a diffusion control, but on closer examination, it appears that the rate controlling mechanism of heterogeneous dissolution reactions is sometimes better predicted from plots of the kinetic equations, rather than the activation energy value [17]. Finally, the linearization of the kinetic curves in Fig. 4 was also carried out by means of equation (1). The values of the rate constants were re-plotted against the reciprocal of the particle radii $({}^{1}/_{r})$, giving a linear relationship with a correlation coefficient of

0.999 (**Fig. 8**). However, the plot of the rate constants as a function of the square of particle radii $\left({}^{1}/_{r^{2}}\right)$ did not give a linear relationship.

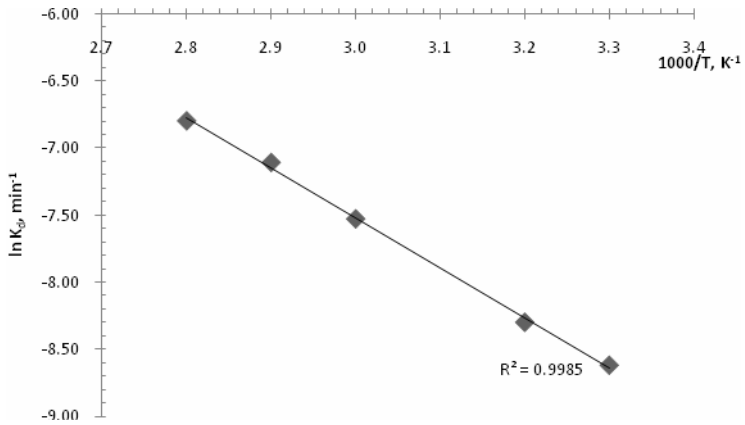

Fig.7 Arrhenius plot of reaction rate, $\ln k_d$ against reciprocal of temperature, 1000/T.

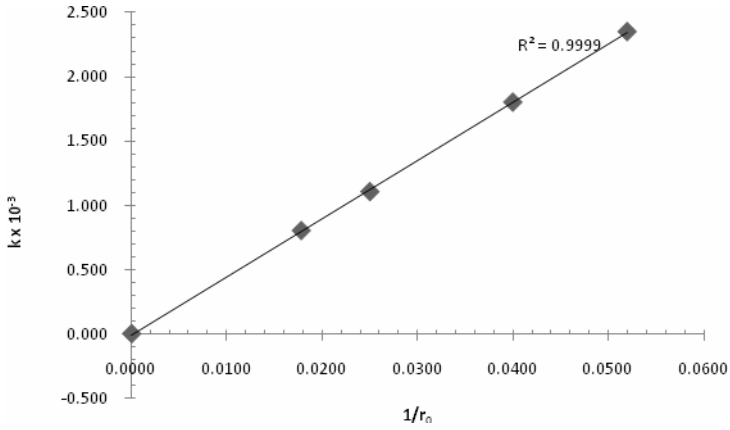

Fig.8 Variation of rate constant, k ($\times 10^{-3}$) on inverse of particle radius, $1/r$

Therefore, the linear dependence of the rate constant on the inverse of particle radius suggests that the surface chemical reaction is the rate controlling step for the dissolution process [18, 19].

3.4 Characterization of reaction products

Several investigators have utilized kinetics models which are based on a reaction which is topochemical in nature. Careful examination and identification of the solid reaction products are important segments of the study of any heterogeneous reaction [20]. To this end, the results of residual product obtained after optimal leaching of spent battery ash in 8.42M at 80^0C is presented in **Fig. 9**.

The leaching residue amounted to about 18% of the initial solid mineral materials shows that the unleached product layer consisting of mainly of silica (α-SiO_2) which and are formed around the

shrinking core of the unreacted materials. It is very interesting to note the absence of lead compounds in the X-ray diffraction of the products layer. However, the purity level of residual product was analyzed for the presence of chloride and other metal ions after washing with doubly distilled water [8].

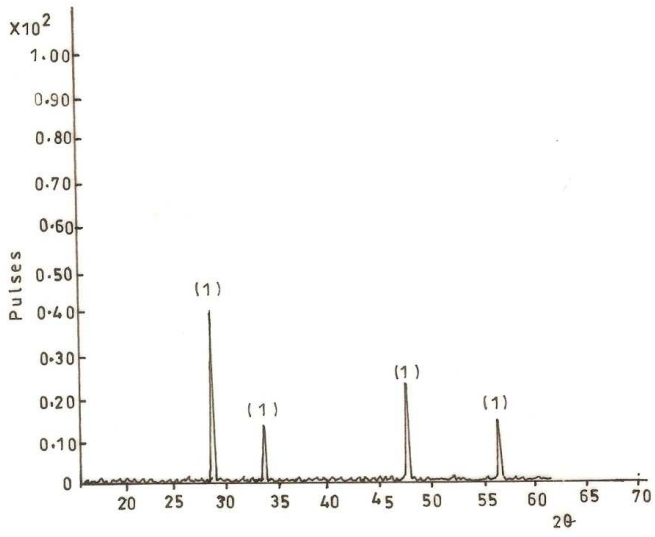

Fig.9 X-ray diffractogram of the residual spent battery ash at 80^0C in 8.42M HCl, showing α-SiO_2 at the major peaks identified at different d-spacing/diffraction peaks (1): α-SiO_2 [46-1045, 1 0 1]

4 Conclusions

In the present study, the dissolution kinetics of the spent motorcycle battery ash was studied in hydrochloric acid. It was found that the dissolution rates increases with increasing hydrochloric acid concentration, temperature, stirring speed and decrease in solid/liquid ratio and particle diameter. The results of the dissolution investigations also indicated that the mechanism of the reaction is diffusion controlled process with surface chemical reaction as the rate controlling step. The reaction order with respect to hydrogen ion [H^+] ion was found to be 0.76. The energy of activation, Ea and Arrhenius constant values of 36.40 kJ/mol and 24.53 s^{-1} were calculated for the process. Finally, the X-ray diffraction spectrum showed that about 18% of the initial solid material that constituted undissolved materials contained silica (α-SiO_2) and its level of purity was evaluated.

References

[1] A.M. Bernades, D.C.R. Espinosa, J.A.S. Tenorio: Journal of Power Sources, Vol. 130, 2004, p. 291-298.
[2] US Patent 5652497. Reconditioning lead acid batteries for optional use in a reverse operational mode. US Patent, 1997.
[3] M.B. Mansur, R.C. Elias, G. Dorella, D.P. Mantuano: Journal of Power Sources, Vol. 159, 2006, p. 1510-1518.
[4] F. Ferella et al.: Acta Metallurgica Slovaca, Vol. 12, 2006, p. 95-104.

[5] D.A. Bertuol, A.M. Bernades, Holeczek, H.J. Fetzer: Acta Metallurgica Slovaca, Vol. 12, 2006, p. 13-19.
[6] J.A.S. Tenorio, C.C.B. Martha-de-Souza: Journal of Power Sources, Vol. 136, 2004, p. 191-196.
[7] A.M. Bernardes, D.C.R. Espinosa, J.A.S. Tenorio: Journal of Power Sources, Vol. 124, 2003, p. 586-592.
[8] A.A. Baba, F.A. Adekola, R.B. Bale: Journal of Hazardous Materials, Vol. 171, 2009, No. 1-3, p. 838-844.
[9] P. Zhang, T. Yokoyama, O. Itabashi, T.M. Suzuki, K. Inoye: Hydrometallurgy, Vol. 47, 1998, p. 259-271.
[10] C.C. Yang: Journal of Power Sources, Vol. 115, 2003, p. 352-359.
[11] D.H. Rubisou, J.M. Krowinkel, V.G. Papangelakis: Hydrometallurgy, Vol. 58, 2000, No. 1, p. 1-11.
[12] G.W. Warren, S. Kim, H.Henein: Metallurgical Transactions B, Vol. 15B, 1986, p. 59-69.
[13] J. Li et. al: Transactions of Nonferrous Metals Society of China, Vol. 19, 2009, p. 751-755.
[14] S. Aydogan, A. Aras, M. Canbazoglu: Chemical Engineering Journal, Vol. 114, 2005, p. 67-72.
[15] O. Levenspiel: Chemical Reaction Engineering, 2nd ed., Wiley, New York, 1972.
[16] A.D. Sousa, P.S. Pina, V.A. Leao, C.A. Silva, P.F. Siqueira: Hydrometallurgy, Vol. 89, 2007, No. 1-2, p. 72-81.
[17] E.O. Olanipekun: Hydrometallurgy, Vol. 96, 1999, p. 39-43.
[18] A.A. Baba, F.A. Adekola, E.E. Toye, R.B. Bale: Journal of Minerals, Materials, Characterization and Engineering, Vol. 8, 2009, No. 10, p. 787-801.
[19] A.A. Baba, F.A. Adekola: Hydrometallurgy, Vol. 101, 2010, No. 1-2, p. 69-75.
[20] J.G. Zuo-mei, W. Warren, H. Henein: Metallurgical Transaction B, Vol. 15B, 1984, p. 5-12.
[21] A.L. Salgado, A.M.O. Veloso, D.D. Pereira, G.S. Gontijo, A. Salum, M.B. Mansur: Journal of Power Sources, Vol. 115, 2003, 367-373.